Mon. Not. R. Astron. Soc. **000**, 1–7 (2004) Printed 20 August 2004 (MN LATEX style file v2.2)

K 4-47: a planetary nebula excited by photons and shocks*

D. R. Gonçalves[1]†; A. Mampaso[1]; R. L. M. Corradi[2]; M. Perinotto[3];
A. Riera[4] and L. López-Martín[1]
[1]*Instituto de Astrofísica de Canarias, E-38205 La Laguna, Tenerife, Spain*
[2]*Isaac Newton Group of Telescopes, Apartado de Correos 321, E-38700 Sta. Cruz de La Palma, Spain*
[3]*Dipartimento di Astronomia e Scienza dello Spazio, Università di Firenze, Largo E. Fermi 5, 50125 Firenze, Italy*
[4]*Departament de Fìsica i Enginyeria Nuclear, Universitat Politécnica de Catalunya, Avenida Víctor Balaguer s/n,*
E-08800 Vilanova i La Geltrú, Spain

Accepted ?. Received ?; in original form ?

ABSTRACT

K 4-47 is an unusual planetary nebula composed of a compact high-ionization core and a pair of low-ionization knots. Long-slit medium-resolution spectra of the knots and core are analyzed in this paper. Assuming photoionization from the central star, we have derived physical parameters for all the nebular components, and the (*icf*) chemical abundances of the core, which appear similar to Type-I PNe for He and N/O but significantly deficient in oxygen. The nebula has been further modelled using both photoionization (CLOUDY) and shock (MAPPINGS) codes. From the photoionization modelling of the core, we find that both the strong auroral [O III] 4363Å and [N II] 5755Å emission lines observed and the optical size of the core cannot be accounted for if a homogeneus density is adopted. We suggest that a strong density stratification, matching the high-density core detected at radio wavelengths and the much lower density of the optical core, might solve the problem. From the bow-shock modelling of the knots, on the other hand, we find that knots' chemistry is also represented by Type-I PN abundances, and that they would move with velocities of 250 - 300 $\mathrm{km\,s^{-1}}$.

Key words: planetary nebulae: individual (K 4-47) - ISM: kinematics and dynamics - ISM: jets and outflows

1 INTRODUCTION

Planetary nebulae (PNe) are known to possess a variety of small-scale structures that are usually in a lower ionization state than the main body of the nebulae. The morphological and kinematic properties of these low-ionization structures (LISs, Gonçalves, Corradi & Mampaso, 2001) vary from type to type, in the sense that LISs can appear in the form of pairs of knots, filaments, jets, and isolated features moving with velocities that either do not differ substantially from that of the ambient nebula, or instead move supersonically through the environment.

The total number of PNe that are known to possess LISs is 55, i.e. about 10% of all the 527 Galactic PNe imaged in filters of high- and low-ionization emission lines (Balick 1987; Schwarz, Corradi & Melnick 1992; Manchado et al. 1996). The different types of LISs may be easily seen in Corradi et al. (1996).

At present, the origin of jets and pairs of knots in PNe is not completely clear. From the theoretical point of view, the principal physical process behind the formation of collimated LISs is the interplay between the stellar AGB and post-AGB winds (for single stars) or between stellar and disk winds (if the central star is binary). According to the various studies dedicated to this issue (e.g. García-Segura 1997; García-Segura & López 2000; Steffen, López & Lim 2001; Blackman, Frank & Welch 2001) jets and knots originated by this interplay are predicted to be supersonic, highly collimated and two-sided. In the case of single stars these are expected to be produced at the same time as the main PN shell, but in the case of a binary star origin they may be younger than the host PN. However, important properties of these LISs such as density contrasts, the peculiar nitrogen abundance and main excitation mechanisms, appear hard to explain (see Dwarkadas & Balick 1998; Balick & Frank 2002; Gonçalves et al. 2003).

K 4-47 (PN G149.0+04.4) is a compact PN that contains LISs. It is composed by a small, high ionization nebular core and a pair of low-ionization, high-velocity knots, connected to the core by a much fainter low-ionization lane

---

* Based on observations obtained at the 2.5 INT telescope of the Isaac Newton Group in the Spanish Observatorio de Roque de los Muchachos of the the Instituto de Astrofísica de Canarias.
† E-mail: denise@ll.iac.es

(Corradi et al. 2000; see Figure 1). Gonçalves et al. (2001) have proposed that the low-ionization lanes and knots of K 4-47 are genuine jets. Their morphological and kinematical properties are explainable if the jets and knots were formed by accretion disks, attaining velocities of several hundred kilometers per second (the main properties of these models are also summarized in Gonçalves et al. 2001 and Balick & Frank 2002). These highly supersonic velocities imply that the resulting LISs are likely to be shock-excited.

K 4-47 is a poorly studied PN, for which statistical methods provide an unrealistic wide range of distances, for instance, 8.5 kpc (Cahn, Kaler & Stanghellini 1992) or 26 kpc (van de Steene & Zijlstra 1994). Corradi et al. (2000) computed a distance between 3 kpc and 7 kpc assuming that the object participates to the ordered rotation of the disk of the Galaxy, but note that the relatively large height of K 4-47 on the Galactic plane (0.54 kpc for a distance of 7 kpc) adds some further uncertainty to this determination. Tajitsu & Tamura (1998) estimated a distance of 5.9 kpc using the integrated IRAS fluxes under the (crude) assumption of constant dust mass for all PNe. Lacking of anything better, we shall adopt in the following this distance of 5.9 kpc. Lumsden et al. (2001) mapped the H_2 emission from K 4-47 finding that it is excited by shocks. The object also appears in the 6 cm VLA radio survey of Aaquist & Kwok (1990) showing a very compact radio core, with a diameter of 0.25 arcsec, and one of the largest brightness temperatures (T_b=8700 K) found in PNe. So far, the properties (luminosity and temperature) of its central star as well as its nebular (physical and chemical) properties are not known.

In this work, we address the debated issue of the nature and origin of high-velocity LISs, through the determination of the physical parameters, excitation and chemistry of K 4-47. Spectra of the core and the pair of knots are analyzed using two different models, which consider the gas to be either fully photoionized by the PN central star, or fully ionized by shocks. We will show that K 4-47 is particularly interesting for this study because, in contrast to most of the LISs studied up to now (Dopita 1997; Dwarkadas & Balick 1998; Miranda et al. 2000; Gonçalves 2003; Gonçalves et al. 2003), its pair of LISs is mainly shock excited.

2 DATA ACQUISITION AND REDUCTION

Spectra of K 4-47 were obtained on 2001 August 28 at the 2.5m Isaac Newton telescope (INT) at the Observatorio del Roque de los Muchachos on La Palma (Spain), using the Intermediate Dispersion Spectrograph (IDS). The IDS was used with the 235 mm camera and the R300V grating, providing a spectral coverage from 3650 Å to 7000 Å with a spectral reciprocal dispersion of 3.3 Å pix^{-1} and a resolution of 6.9 Å. The spatial scale of the instrument was $0''.70$ pix^{-1} with the TEK5 CCD. Seeing varied from $1''.1$ to $1''.2$. The slit width and length were $1.5''$ and $4'$, respectively. The slit was positioned through the centre of the nebula at P.A. = 41°, passing through the knots, and the exposure times were 3×1800 s.

Bias frames, twilight and tungsten flat-field exposures, arcs and exposures of standard stars BD+332642, Cyg OB2#9, HD19445, and BD+254655, were obtained. Spectra were reduced and flux calibrated using the standard IRAF package for long-slit spectra. Line fluxes were measured separately for the three nebular regions indicated in Figure 1, namely Knot1, Core and Knot2. The observed line fluxes are given in Table 1. Errors in the fluxes were calculated taking into account the errors in the measurement of the fluxes, as well as systematic errors of the flux calibrations, background determination, and sky subtraction. The bottom lines of Table 1 give the estimated accuracy of the measured fluxes for a range of line fluxes (relative to Hβ) in each of the regions. Absolute Hβ fluxes integrated along the slit in each region are as follows: F(Hβ)$_{\rm Knot1}$=2.41; F(Hβ)$_{\rm Core}$=2.76; and F(Hβ)$_{\rm Knot2}$=1.64 (in units of 10^{-15} erg cm^{-2} s^{-1}).

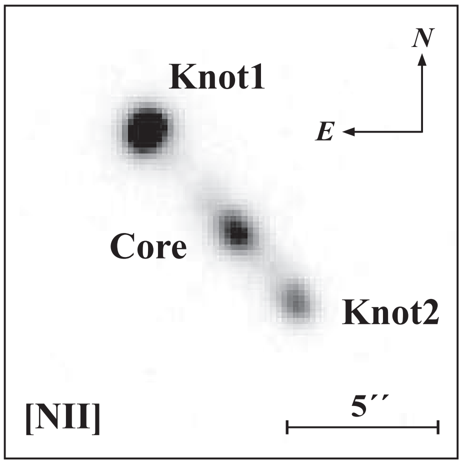

Figure 1. [N II] 6583Å image of K 4-47, adapted from Corradi et al. (2000). Labels of the selected structures are indicated.

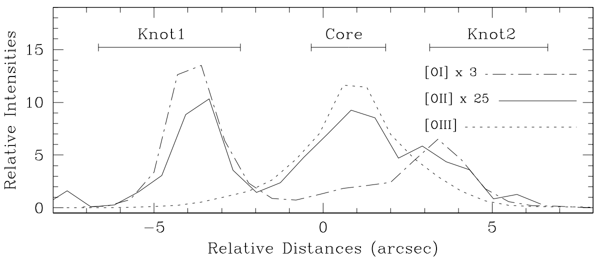

Figure 2. Spatial intensity profile of [O I] 6300Å, [O II] (3726Å+3729Å) and [O III] 5007Å emission lines along P.A.=41°.

3 PHYSICAL PARAMETERS AND DIAGNOSTIC DIAGRAMS

Figure 2 shows the spatial profiles of low- to high-excitation oxygen emission lines ([O I] 6300Å, [O II] (3726Å+3729Å) and [O III] 5007Å); we clearly see that the knots have a much lower excitation than the core. While the low-ionization profiles ([O I] 6300Å and [O II] (3726Å+3729Å)) show local maxima at the positions of the knots, the [O III] 5007Å profile presents its maxima in the core and does not peak at the knots. The average values of [N II] 6583Å/Hα at the knots are 2.0 (Knot1) and 2.1 (Knot2), much higher than those usually found for spherical and elliptical PNe (e.g., Aller & Czyzak 1983), although such values are frequently found in the Peimbert Type I objects (Peimbert 1978; Peimbert & Torres-Peimbert 1983). The Core, on the other hand, has a less extreme [N II] 6583Å/Hα line ratio, 1.2, even though still higher than in most PNe. Peculiar line ratios like those found in K 4-47 have been interpreted as indicative of the presence of shock-excitation or anomalous abundances (see, for instance, Miranda & Solf 1992).

Fluxes were extinction-corrected using $c_{\mathrm{H}\beta}$ (the logarithmic ratio between observed and dereddened Hβ fluxes), determined from the observed Hα/Hβ and Hα/Hγ ratios, for each of the selected features of the nebula, and the reddening law of Cardelli, Clayton, & Mathis (1989). The derived $c_{\mathrm{H}\beta}$ are: 1.26±0.23(Knot1); 1.37±0.17(Core); 1.11±0.17(Knot2). The physical properties (for all the nebular regions) and chemical abundances of the Core were then evaluated assuming pure photoionization by the central star.

3.1 Density and Temperatures

We estimate the electron densities of K 4-47, which are listed in Table 1, using the [S II] 6717Å/6731Å line ratio. Both knots are denser than the core (1900 cm^{-3}) by factors of 2.4 and 1.2 for Knot1 and Knot2, respectively.

Adopting these densities, electron temperatures are estimated using standard line ratios: T_e[O III] is obtained from the [O III] 4959Å/4363Å line ratio, which is appropriate to zones of medium to high excitation, and T_e[N II] from [N II] 6583Å/5755Å, representative of low-excitation regions. The T_e[O III] for Knot1 and the T_e[N II] of the Core, are lower limits. We find that, within the errors and when both determinations are available, the two temperatures are similar. Errors on T_e[O III] at the position of the knots are significantly higher than those of the [N II] temperatures simply because of the low-ionization nature of these regions. Note that T_e is remarkably higher than the typical values for PNe of around 10^4 K (Kaler 1986).

3.2 Diagnostic Diagrams

Figure 3 shows several diagnostic diagrams which are commonly used to distinguish photoionized nebulae from shock-excited objects, adapted from Sabbadin, Minello & Bianchini (1977) and Phillips & Cuesta (1999). In all of them, the knots of K 4-47 are located close to the shock-excited zones while the core is displaced toward the locus where PNe are usually found, i.e. photoionized objects. This suggests that shock-excitation plays an important role in the knots, but not in the core. The fact that in the [O III] (4959Å+5007Å)/Hα *vs.* [S II] (6716Å+6731Å)/Hα diagram Knot2 do not fall exactly within the "Shock Regime" area is not against this interpretation, as its boundaries were originally computed for young stellar objects, using parameters (gas abundances and shock velocities) which can be different from those of evolved objects like K 4-47.

The large expansion velocities of the knots and their broadened line profiles (Corradi et al. 2000) are also typical of shocked flows like H-H objects. In addition, the shock-excited nature of the knots would be consistent with their measured T_e (Table 1), unusually large for low-ionization microstructures in PNe, and with their extremely high [N II] 6583Å/Hα line ratio. On the contrary, the velocities observed in the core are substantially lower than in the knots, and so is its [N II] 6583Å/Hα line ratio.

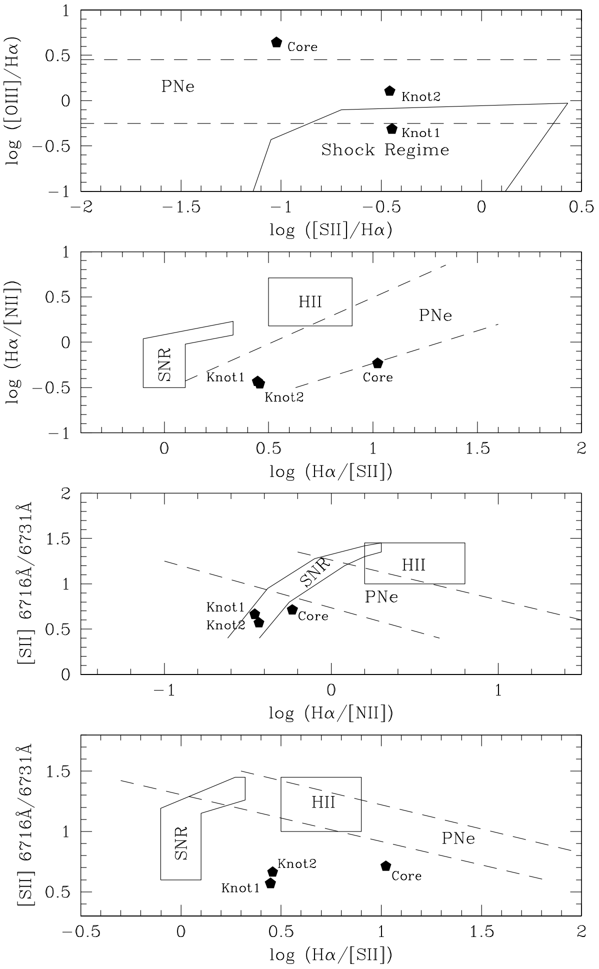

Figure 3. Diagnostic diagrams showing the loci of the core and knots in K 4-47. They include the empirical loci of the PNe, supernova remnants (SNR) and HII regions (HII), as well as the theoretical "Shock Regime" zone as defined by Phillips and Cuesta (1999) using the plane-parallel and bow-shock models of Hartigan, Raymond & Hartmann (1987). Line ratios considered are the sum of the doublets ([O III]≡[O III] 4959Å+5007Å; [S II]≡[S II] 6716Å+6731Å; [N II]≡[N II] 6548Å+6583Å) when not followed by the specific wavelength.

It is therefore suggested that the high velocity knots Knot1 and Knot2 of K 4-47 are mainly shock heated, while the Core is mainly photoionized. With the aid of existing photoionization and shock modelling we will explore in the following these alternatives.

4 ANALYSIS OF THE CORE

4.1 Empirical Abundances

Ionic and total abundances for the Core were computed using the ionization correction factors (*icf*) scheme, following Kingsburgh & Barlow (1994), as described in Corradi et al. (1997) and Gonçalves et al. (2003). Results are shown in

Table 2. Note that as the T_e[N II] in Table 1 is only a lower limit, the abundances of the low-ionization ions are upper limits. Errors on the total abundances are obtained by propagating the errors in the ionic abundances as well as on the *icf*, and are indicated within brackets in the table as percentage errors (14% for He, for which no *icf* is applied, and 30–50% for O and N).

According to its large He and N/O abundances, K 4-47 is similar to most bipolar PNe (Perinotto & Corradi 1998), and would be classified as a Type I PN (Peimbert & Torres-Peimber 1983, see also Kingsburgh & Barlow 1994). However, the O, Ne and S abundances of K 4-47 are among the lowest measured for Galactic PNe, and are more typical of some halo (or Type IV) PNe (see e.g. Howard, Henry & McCartney 1997).

High He/H abundances ($0.15 \leqslant$ He/H $\leqslant 0.20$), and some (but much less extreme than in K 4-47) oxygen deficiency ($1.35 \leqslant$ O/H ($\times 10^{-4}$) $\leqslant 2.7$), were found in other bipolar PNe, such as NGC 6302 (Pottasch & Beintema 1999), NGC 6537 and He 2-111 (Pottasch, Beintema & Feibelman 2000). Very much like in the case of K 4-47, these PNe have considerably high electron temperatures (average T_e, from optical, ISO and IUE spectra for the three of them are 17200 K up to 18300 K). Therefore, we have the somewhat contradictory result that while K 4-47 seems to be an extreme bipolar PN in terms of its morphology and He and N abundances, its O, Ne and S abundances rather resemble PNe in the Galactic halo, as its relatively large height on the Galactic plane might also suggest (see Section 1), and contrary to bipolar PNe which are highly concentrated toward the Galactic plane (Corradi & Schwarz 1995).

To further investigate these issues, in the next two Sections we will model the Core spectrum using, first, a shock excitation code, and, then, a pure photoionization model.

4.2 Plane-parallel Shock Modelling

Shock models have successfully reproduced the emission line ratios, line profiles and, recently, velocity maps in HH objects (Beck et al. 2004). To check the possible influence of shock excitation on the Core spectrum we have explored a variety of steady plane-parallel models, for which we use the photoionization-shock code MAPPINGS Ic (Dopita, Binette & Tuohy 1984; Binette, Dopita & Tuohy 1985).

One important characteristic of shock models is that the predicted spectra strongly depends on the preshock ionization. We have compiled a set of fully pre-ionized shock models (i.e. the incident gas has been ionized) and a set of local equlibrium preionization for the gas entering the shock (as described by Shull & McKee 1979, Hartigan et al. 1987). Relative abundances typical of Type I PNe were assumed, and two values for the pre-shock density were considered (100, 1000 cm^{-3}). The input shock velocities were varied from 95 to 140 km s^{-1}, i.e. the range producing large [O III] (4959Å,5007Å)/Hβ ratios (Hartigan et al. 1987), as observed. Note, however, that the measured expansion velocity of the Core is smaller than 50 km s^{-1} (Corradi et al. 2000), pointing to lower shock velocities.

None of the predicted spectra could reproduce the large observed ratios of intermediate to high excitation emission lines with respect a H I Balmer line (i.e. [O II] 3727Å/Hβ, [O III] 5007Å/Hβ, [Ne III] 3868Å/Hβ and He II 4686Å/Hβ). Moreover, the shocked spectra predicted by our models imply [O I] 6300Å/Hα and [S II] (6716Å+6731Å)/Hα larger than the observed values. A large discrepancy was also found with the observed [O III] 4959Å/4363Å emission line ratio, which is more than 2 times larger than the model values. And, finally, [N II] 6583Å/5755Å is very high, ≈ 300, because the intensity of [N II] 5755Å is largely understimated by these models.

We conclude that the plane-parallel shock models are not able to reproduce the spectrum of the core of K 4-47.

4.3 Photoionization Modelling

We have used the photoionization code CLOUDY 95.06 (Ferland et al. 1998).

CLOUDY needs as input the information on the shape and intensity of the radiation from the ionizing source, the chemical composition and geometry of the nebula, as well as its density and size. As mentioned in Section 1, the distance of K 4-47, and thus its size and the luminosity of the central star, are poorly known. We adopt the distance of 5.9 kpc computed by Tajitsu & Tamura (1998), although extending the calculations to the full range of distances from 3 kpc to 7 kpc proposed by Corradi et al. (2000).

A spherical geometry, and a filling factor of 1.0 have been assumed. Using the Hα and [N II] images from Corradi et al. (2000) a core diameter of 1.9 arcsec was estimated (10% contour extension corrected for the finite resolution; Tylenda et al. 2003). The density was initially kept to constant and equal to its empirical value (1900 cm^{-3}, see Table 1). However, as noted in the Introduction, Aaquist & Kwok (1990) discovered a bright and very compact radio core at the centre of K 4-47, implying a high density of 72000 cm^{-3} (assuming an optically thin nebula at 5 GHz, the distance of 5.9 kpc and following Goudis 1982). For this reason, models with much higher density values were also explored.

Dust grains have been included, since they have an important effect, particularly on the temperature structure of PNe. This effect depends on the type of grain (graphite and/or silicate), the grain abundances, and the grain-size distribution, being more relevant in the inner regions of the nebula (see Dopita & Sutherland 2000). Both graphite and silicate grains were considered. As we do not know the grain size distribution and grain abundances for K 4-47 and more in general for PNe, we adotped ISM size distribution, with ISM gas-phase depletions due to grains, following van Hoof et al. (2004).

We adopted a blackbody spectrum for the central star, with T_{eff} derived from the Hβ, HeI and HeII emission line ratios, using a modified Zanstra method as done for instance by Mikołajewska et al. (1999). This gives T_{eff}=130 000 K (from HeII 4686Å/Hβ) and T_{eff}=115 000 K (from HeII 4686Å/HeI 5876Å). A lower limit to the central star luminosity comes from the IRAS spectral energy distribution (Tajitsu & Tamura 1998), which gives L$\geqslant$ 16 D^2 $L_\odot$ (where D is the distance in kpc) yielding 550 $L_\odot$ at 5.9 kpc.

As with the elemental abundances, we first run models with the empirical abundances given in Table 2, and subsequently with “average” values for either normal (Type-II), or Type-I PNe, following Kingsburgh & Barlow (1994). CLOUDY models with the empirical abundances do not match the observed line fluxes. Both helium and [N II] (6548Å,6583Å) emission lines are largely overestimated, while oxygen, sulphur and neon lines are underestimated, mainly because the very low O/H, Ne/H and S/H input abundances are not compensated by a high electron temperature in the model as empirically determined. Tests with Type-II PNe abundances were also not successful because the predicted [N II] 6548Å,6583Å intensities are very low, which is expected as the main difference between Type-I and Type-II abundances is that the latter are depleted in nitrogen by a factor of ∼4 (Kingsburgh & Barlow 1994). Assuming Type-I abundances, we found a partial agreement with the observed spectrum for T_{eff}=120 000 K, L=550 $L_\odot$ and N$_e$= 1900 cm^{-3}. Important optical lines like HeII 4686Å, [O III] (4959Å,5007Å), [N II] (6548Å,6584Å) and [S II] (6716Å,6731Å) are well reproduced by this model, with discrepancies of 10% or less. HeI 4471Å, 6678Å, HeII 5412Å, and [S III] 6312Å lines agree with the observed spectrum within 12% to 20%. Other relatively intense lines such as [O II] (3726Å+3729Å), [NeIII] 3868Å, and HeI 5876Å show discrepancies of 35% to 50% with respect to the model. Furthermore, the model underestimates the intensities of the [O III] 4363Å and the [N II] 5755Å lines by a factor of about 3. These lines are the keys for the determination of the electron temperature. Finally, the model underestimates [NI] 5200Å and [OI] 6300Å by factors larger than 30. Let us note, in addition, that this model requires a size for the core of 4.0 arcsec, twice the optical size observed.

It is then instructive to explore alternative scenarios. Let us first note that in some PNe and related objects (see e.g. Corradi 1995), high [O III] 4363Å and [N II] 5755Å line intensities have been interpreted as the signature of very high core densities, as at N_e larger than about 10^5 cm^{-3} the auroral ([O III] 4363Å and [N II] 5755Å) to nebular ([O III] 4959Å and [N II] 6583Å) line ratios are indicators of density rather than of temperature (Gurzadyan 1970). For this reason, we have calculated other models assuming much higher (albeit still constant) densities. As noted above, high core densities are implied by the radio size and flux (Aaquist & Kwok 1990).

CLOUDY models for the observed radio core size, 0.25 arcsec, and such high densities (from 72000 K up to 3.0×10^5cm^{-3}) show that both [O III] 4363Å and [N II] 5755Å intensities can be now reproduced, but other nebular lines, in particular [O II] (3726Å+3729Å), [N II] (6548Å,6583Å), and [S II] (6717Å,6731Å), become now largely underestimated because of collisional quenching. A natural way to solve the problem might be to assume a strong density stratification in the core of K 4-47, with a very dense inner zone where [O III] 4363Å and [N II] 5755Å are mostly formed, and a lower density outer region where other important nebular lines are produced. This idea should be tested by means of an appropriate photoionization model; 3-D codes (like MOCASSIN; Ercolano et al. 2003) are much better suited than CLOUDY to deal with such extreme density variations.

In summary, we find that none of the constant density models is able to account, simultaneouly, for all optical emission lines in the Core. In particular, the [O III] 4363Å and [N II] 5755Å intensities are strongly understimated if the nebular density is the one derived empirically from the [S II] lines. A model with a strong density stratification could possibly offer a solution to the problem.

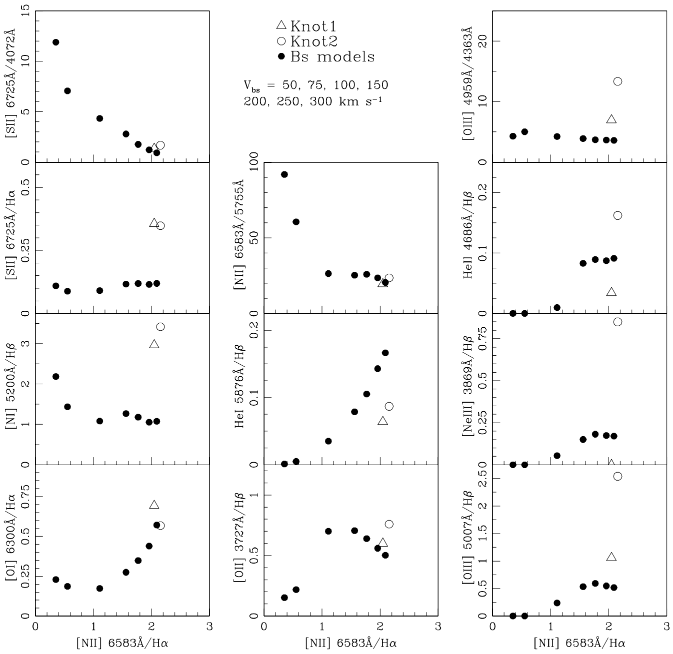

Figure 4. Results of the bow-shock models, in terms of line ratios, as compared to the observed emission. Results are shown for bow-shock velocities of V$_{bs}$ of 50, 75, 100, 150, 200, 250, and 300 km s^{-1}, corresponding to points moving from left to the right side inside each panel.

5 SHOCK MODELLING FOR THE KNOTS

The fact that we are not able to provide an accurate representation of the Core spectrum, also prevents us to determine the radiation escaping from the core and reaching the knots, and thus to attempt a reliable photoionization modelling of the latter. A consistent photoionization modelling of the whole nebula (core+knots) would also require a fully 3-D modelling, that goes beyond the scopes of the present work. Given the evidence that the knots might be excited by shocks (Section. 3.2), we instead attempt to describe their spectrum using existing shock models.

5.1 Bow-Shock Models

We have used the bow-shock models described in Raga & Bohm (1986) and Hartigan et al. (1987). We consider a bow shock with a functional form, $z/a = (r/a)^p$, where z is measured along the symmetry axis, r is the cylindrical radius, the parameter p determines the shape of the bow shock and the constant a determines its size (Beck et al. 2004). The emission from the bow-shock is modeled as described by Hartigan et al. (1987), being the geometry of the bow shock the parameter that determines the shock velocity.

The plane-paralel shock models required to predict the bow-shock emission line ratios are obtained with the photoionization-shock code MAPPINGS Ic. We have adopted a pre-shock density of 400 cm^{-3}, that is within the range generally assumed for stellar jets. The pre-shock magnetic field was taken to be negligible. We assumed elemental abundances for He, C, N, O, Ne, S, and Ar to be within the range of Type-I PN values. As for the preionization of the gas, local equilibrium is assumed. We consider the bow-shock velocity as a free parameter, adopting a set of values from 50 to 300 km s^{-1}.

5.2 Comparison with the Observed Spectra

We have obtained the best fit to the observed spectra for p=3. A summary of the results is presented in Figure 4 for a number of emission line ratios plotted as a function of [N II] 6583Å/Hα. Note that the later line ratio increases in strength as the shock velocity increases, and in the case of K 4-47 is matched by only the largest shock velocities considered, somewhat larger than the estimate of 150 km s^{-1} by Corradi et al. (2000).

For these velocities, the bow-shock models fit pretty well the line ratios [S II] (4069Å+4076Å)/(6717Å+6731Å)≡[S II] 4072Å/6725Å, and [N II] 6583Å/5755Å, sensitive to the temperature in the recombination zone where [S II] and [N II] are formed, but not equally well the [O III] 4959Å/4363Å ratio, indicating that the predicted electron temperature T_e[O III] is too large. The [N II] and [O III] electron temperatures predicted by these models, for both knots, are 17800 K and 27600 K, respectively.

The ratios [O I] 6300Å/Hα and [O II] (3726Å+3729Å)/Hβ are also well reproduced. Larger discrepancies appear for the helium lines HeI 5876Å and HeII 4686Å, and specially for [Ne III] 3868Å and [O III] 5007Å in Knot2, and [S II] (6716Å+6731Å) and [N I] 5200Å in both knots. Note that a similar problem for the [S II] (6717Å+6731Å)/Hα ratio is also found in HH objects (Raga et al. 1996). The large discrepancy for the [N I] 5200Å/Hβ emission line ratio is intriguing, as strong line intensities for this ion can only be produced with low shock velocities, which could however not account for the observed flux of higher ionization stages like [N II] 6583Å. Different shock geometries, producing a different distribution of shock velocities, might help to solve this problem.

Also note that the bow-shock models are based on appraisal of what would be reasonable parameters for the knots of K 4-47, and we did not intend to reproduce the line intensities separately for each of the knots. But the knots are not identical: in particular, high excitation lines like HeII 4686Å, [Ne III] 3868Å and [O III] 5007Å are much brighter in Knot2 than in Knot1, which indicates that the radiation field of the central star would affect the Knot2 emission line spectrum much more than that of Knot1. The observed spectra of Knot2 would also fit a model with a somewhat larger N/H abundance and a lower bow shock velocity.

Summarising, the analysis of the shock-excited knots suggests that they are high-velocity (250 to 300 km s^{-1}) condensations with high electron temperatures (T_e[N II] =17800 K) and chemical abundances similar to Type-I PNe.

6 DISCUSSION

The analysis presented in this paper is the first attempt to determine the physical parameters, excitation mechanism and chemical abundances of K 4-47. Among other PNe with LISs, M 2-48 (López-Martín et al. 2002) and Kj Pn 8 (López, Vázquez & Rodríguez 1995) have, similarly to K 4-47, a high electron temperature and the evidence for shock-excited LISs. But note that in these PNe, except for one of the M 2-48's knots (for which T_e is 20100 K, twice the core temperature), T_e and N_e are not estimated in a detailed zone-by-zone basis, because [O III] 4363Å and [N II] 5755Å were not measured.

The two distinct models that we used for the analysis of K 4-47 (pure photoionization for the core and pure shock-excitation for the pair of knots), provide some clues for the interpretation of this nebula.

First, the analysis of the core would suggests He and N overabundances typical of Type-I (Galactic disk) PNe, but also an extreme oxygen deficiency which is instead more typical of PNe in the Galactic halo. These abundances calculation would however be invalidated if more detailed modelling proves the existence of a strong density stratification within the core, with an inner region with extremely high density ($\sim 10^5$ cm^{-3}), and an outer zone with a much lower density matching the empirical determination from the [S II] lines. In fact, in this case the T_e determined empirically using the [O III] 4959Å/4363Å and [N II] 6583Å/5755Å line ratios would be wrong, as the auroral and nebular lines involved would be formed in different regions. Note that, albeit unusual, such high density cores were actually found in several other PNe (Corradi 1995), which like K 4-47 show an extreme degree of collimation.

Second, the knots seem to be mainly shock-excited. This conclusion is strenghtened by diagnostic line ratio diagrams, and, interestingly, by the fact that the H_2 emission of K 4-47 is also shock-excited, contrary to most PNe where instead it is excited by fluorescence (Lumsden et al. 2001). Our shock modelling also indicates that knots have Type-I abundances. According to these models, knots would move with space velocities of 250-300 km s^{-1}, about twice the value estimated by Corradi et al. (2000) from the analysis of the lines profiles. Moreover, while the shock model is successful in matching the [N II] (6583Å/5755Å) line ratio at the knots it underestimate their [O III] (4959Å/4363Å) ratio by some 30% and 70% for Knot1 and Knot2, respectively.

As a final remark, the two physical processes explored separately in this paper, i.e. photoionization and shock heating, are likely to be simultaneously present in a real nebula like K 4-47, as gas can be ionized by both energetic photons from the central star and from the shocks associated with the observed supersonic outflows. Taking this into account would require a sophisticated modelling which is not presently available, and which would also need to be supported by a better knowledge of the nebular and stellar parameters. In particular, very little information is presently known about the distance and the properties of the central star of K 4-47, a basic data that could be addressed by future observations.

ACKNOWLEDGMENTS

We thank the anonymous referee for his/her comments, which helped us to improve the paper significantly. We also thank Joanna Mikołajewska for fruitful discussions and Corrado Giammanco for helping with CLOUDY. The work of DRG, AM, RLMC and LLM is partially supported by a grant from the Spanish Ministry of Science and Technology (AYA 2001-1646). The work of AR is supported by the grant AYA 2002-00205.

REFERENCES

Aaquist, & Kwok, S. 1990, A&AS, 84, 229

Aller, L. H., & Czyzak, S. J. 1983, ApJS, 51, 211

Balick, B. 1987, AJ, 94, 671

Balick, B.; & Frank, A. 2002, ARA&A, 40, 439

Blackman, E. G., Frank, A., & Welch, C. 2001, ApJ, 546, 288

Beck, T. L., Riera, A., Raga, A. C. & Aspin, C. 2004, AJ, 127, 408

Binette, L., Dopita, M. A. & Tuohy, I. R. 1985, ApJ, 297, 476

Cahn, J. H., Kaler, J. B., & Stanghellini, L. 1992, A&AS, 94, 399

Cardelli, J. A., Clayton, G. C., & Mathis, J. S. 1989, ApJ, 345, 245

Corradi, R. L. M. 1995, MNRAS, 276, 521

Corradi, R. L. M., Schwarz, H.E., 1995, A&A 293, 871

Corradi, R. L. M., Manso, R., Mampaso, A., & Schwarz, H. E. 1996, A&A, 313, 913

Corradi, R. L. M., Perinotto, M., Schwarz, H. E., Claeskens, J.-F. 1997, A&A, 322, 975

Corradi, R. L. M., Gonçalves, D. R., Villaver, E., Mampaso, A., Perinotto, M., Schwarz, H. E., & Zanin, C. 2000, ApJ, 535, 823

Dopita, M. A. 1997, ApJ, 485, L41

Dopita, M. A., Binette, L. & Tuohy, I. R. 1984, ApJ, 282, 142

Dopita, M. A., & Sutherdland, R. S. 2000, ApJ, 539, 742

Dwarkadas, V. V., & Balick, B. 1998, ApJ, 497, 267

Ercolano, B., Barlow, M. J., Storey, P. J., & Liu, X.-W. 2003, MNRAS, 340, 1136

Ferland G. J., Korista K. T., Verner D. A., Ferguson J. W., Kingdon J. B., Verner E. M., 1998, PASP, 110, 761

García-Segura, G. 1997, ApJ, 489, L189

García-Segura, G., & López, J. A. 2000, ApJ, 544, 336

Gonçalves, D. R., Corradi, R. L. M., & Mampaso, A. 2001, ApJ, 547, 302

Gonçalves, D. R. 2003, in Asymmetric Planetary Nebulae III, Eds. M. Meixner, J. Kastner, B. Balick and N. Soker, ASP Conf. Series, in press, astro-ph/0312527

Gonçalves, D. R., Corradi, R. L. M., Mampaso, A., & Perinotto, M. 2003, ApJ, 597, 975

Goudis, C.: 1982, 'The Orion complex: A case study of interstellar matter' (Appendix II), Reidel, Dordrecht

Gurzadyan, G. A.: 1970, 'Planetary Nebulae', Reidel, Dordrecht

Hartigan, P., Raymond, J., & Hartmann, L. 1987, ApJ, 316, 323

Howard, J. W., Henry, R. B. C., McCartney, S. 1997, MNRAS, 284, 465

Kaler, J. B. 1986, ApJ, 308, 322

Kingsburgh, R. L., & Barlow, M. J. 1994, MNRAS, 271, 257

López, J. A., Vázquez, R., & Rodríguez, L. F. 1995, ApJ, 455, L63

López-Martín, L., López, J. A., Esteban, C., Vázquez, R, Raga, A., et al. 2000, A&A, 388, 652

Lumsden, S. L., Puxley, P. J., & Hoare, M. G. 2001, MNRAS, 328, 419

Manchado, A., Guerrero, M. A., Stanghellini, L., & Serra-Ricart, M. 1996, The IAC Morphological Catalog of Northern Galactic PNe, IAC Publ.

Mikołajewska, J., Brandi, E., Hack, W., Whitelock, P. A., Barba, R., García, L., & Marang, F. 1999, MNRAS, 305, 190

Miranda, L. F., & Solf, J. 1992, A&A, 260, 397

Miranda, L., et al., 2000, MNRAS, 311, 748

Peimbert, M. 1978, IAU Symp. 76, Planetary Nebulae, ed. Y. Terzian (Reidel, Dordrecht), p. 215

Peimbert, M., & Torres-Peimbert, S. 1983, IAU Symp. 103, Planetary Nebulae, ed. D. R. Flower (Kluwer, Dordrecht), p. 233

Perinotto, M., Corradi, R. L. M. 1998, A&A, 332, 721

Phillips, J. P., & Cuesta, L. 1999, AJ, 118, 2919

Pottasch, S. R., Beintema, D. A., & Feibelman, W. A. 2000, A&A, 363, 767

Pottasch, S. R., & Beintema, D. A. 1999, A&A, 347, 975

Raga, A. C. & Böhm, K. H. 1986, ApJ, 308, 829

Raga, A. C., Böhm, K. H. & Cantó, J. 1996, RMxAA, 32, 161

Sabbadin, F., Minello, S., & Bianchini, A. 1977, A&A, 60, 147

Schwarz, H. E., Corradi, R. L. M.; & Melnick, J. 1992, A&AS, 96, 23

Shull, J. M. & McKee, C. F. 1979, ApJ, 227, 131

Steffen, W., López, J. A., & Lim, A. 2001, ApJ, 556, 823

Tajitsu, A., & Tamura, S. 1998, AJ, 115, 1989

Tylenda, R., Siódmiak, N., Górny, S. K.,Corradi, R. L. M., & Schwarz, H. E. 2003, A&A, 405, 627

van Hoof, P. A. M., Weingartner, J. C., Martin, P. G., Volk, K., & Ferland, G. J. 2004, MNRAS, 350, 1330

van de Steene, G. C., & Zijlstra, A. A. 1994, A&AS, 279, 521

This paper has been typeset from a TEX/ LATEX file prepared by the author.

Table 1. Observed emission line fluxes (normalized to Hβ =100), electron density and temperatures. The estimated percentage errors in the line fluxes (for a range of fluxes relative to Hβ) are given at the bottom.

	Line Fluxes		
Line Identification (Å)	Knot1	Core	Knot2
[O II] 3726.0 + 3728.8	23.4	26.6	33.3
H9 3835.4	9.45	-	-
[Ne III] 3868.7	-	48.9	40.3
He I 3888.7 + H8 3889.1	-	7.05	12.8
[Ne III] 3967.5 + Hϵ 3970.1	11.5	38.9	27.8
[S II] 4068.6	23.1	3.18	20.0
[S II] 4076.4	15.0	2.49	10.7
Hδ 4101.8	15.6	16.1	16.6
Hγ 4340.5	30.1	32.0	27.8
[O III] 4363.2	3.45	20.8	4.56
He I 4471.5	-	4.28	9.22
N III + O II 4641.0	3.69	4.40	-
He II 4685.7	2.95	24.4	14.3
Hβ 4861.3	100	100	100
[O III] 4958.9	35.9	361	100
[O III] 5006.86	118	1088	279
[N I] 5200.2	367	42.0	421
He II 5411.6	-	4.11	-
[O I] 5577.4	12.6	-	10.4
[N II] 5754.6	51.4	43.6	40.3
He I 5875.7	11.5	42.5	14.6
He II 5882.0	-	-	5.54
He II 5896.5	5.82	-	10.1
[O I] 6300.3	427	54.7	305
[S III] 6312.1	-	7.65	-
[O I] 6363.8	146	17.1	99.1
[N II] 6548.0	446	333	415.2
Hα 6562.8	681	762	587.8
[N II] 6583.4	1406	976	1276
He I 6678.1	3.22	13.4	-
[S II] 6716.5	93.5	32.1	86.0
[S II] 6730.8	165	45.2	130
N_e[S II](cm^{-3})	4600±850	1900±420	2400±400
T_e[O III](K)	$\geqslant$21000	19300±2300	16100±4400
T_e[N II](K)	18900±2950	$\geqslant$21000	16950±2800

	Percentage errors in line fluxes		
Line Fluxes	Knot1	Core	Knot2
(0.01–0.05)$I_{H\beta}$	51	41	58
(0.05–0.15)$I_{H\beta}$	23	15	26
(0.15–0.30)$I_{H\beta}$	14	11	15
(0.30–2.0)$I_{H\beta}$	12	8	11
(2.0–5.0)$I_{H\beta}$	12	7	9
(5.0–10.0)$I_{H\beta}$	11	7	9
$>$ 10 $I_{H\beta}$	11	7	9

Table 2. Ionic and total abundances of the Core. Percentage errors are given within brackets.

Elemen/Iont	Abundances
He^{+}/H	1.14E-01(08)
He^{2+}/H	2.56E-02(14)
He/H	**1.39E-01(14)**
O^{0}/H	5.10E-06(10)
O^{+}/H	3.09E-06(14)
O^{2+}/H	6.13E-05(21)
icf(O)	1.14
O/H	**7.37E-05(32)**
N^{0}/H	8.47E-06(14)
N^{+}/H	1.57E-05(8)
icf(N)	23.8
N/H	**3.74E-04(40)**
Ne^{2+}/H	1.44E-05(32)
icf(Ne)	1.20
Ne/H	**1.74E-05(66)**
S^{+}/H	2.24E-07(14)
S^{2+}/H	7.44E-07(36)
icf(S)	2.02
S/H	**1.96E-06(48)**